Check for updates

Chemistry–A European Journal
Research Article
doi.org/10.1002/chem.202400354
Chemistry Europe
European Chemical Societies Publishing
www.chemeurj.org

Synthesis and Structure of the Small Superelectrophile $[C_2(OH)_2Me_2]^{2+}$

Alan Virmani,[a] Christoph Jessen,[a] and Andreas J. Kornath*[a]

The acid-activation of 1,2-dicarbonyl compounds plays a key role in a variety of electrophilic reactions, some of which are only accessible in superacidic media when a superelectrophilic dication is formed. To obtain structural and electronic information about these elusive species, the vicinal dication $[C_2(OH)_2Me_2]^{2+}$ is synthesized and characterized by Raman spectroscopy and X-ray diffraction. Since this superelectrophile could not be stabilized in convenient superacids, the usage of liquid SO_2 turned out to be crucial. The experimental data are discussed together with quantum-chemical calculations on the B3LYP/aug-cc-pVTZ level of theory. Natural Bond Orbital (NBO) analyses quantify the superelectrophilic interactions found in the solid state.

Introduction

The properties of the ethylene dication, the simplest vicinal carbon-centered superelectrophile, have been a subject of interest for a long time, especially in terms of geometry, charge repulsion, and the influence of substituents in the case of its derivatives.[1–3] *Schleyer* and others calculated different geometries of the parent compound $[C_2H_4]^{2+}$ and found that the perpendicular D_{2d} structure is the most efficient way to delocalize the vicinal positive charges.[4–6] *Frenking* compared different geometries of substituted ethylene dications of the formula $[C_2X_2Y_2]^{2+}$ (X, Y = F, OH, NH_2, SH).[7] He concluded that the introduction of second-row substituents led to a planar structure due to the overlap of π-orbitals and hence an electron-donating effect on the CC(π) bond, provided the steric repulsion of the substituents is not too strong. To generate and stabilize superelectrophiles in the condensed phase, superacids are one of the most efficient tools. The first stable carbon-centered dications synthesized in the condensed phase contained large aromatic substituents to distribute the positive charges over the whole molecule.[8,9] In a recent study, we were able to determine the crystal structure of $[C_2(OH)_3Me][SbF_6]_2 \cdot HF$ by diprotonation of pyruvic acid and discussed the geometry of the carbon scaffold.[10]

Shudo et al. investigated acid-catalyzed reactions of selected 1,2-dicarbonyl compounds like 2,3-butanedione with benzene, leading to geminal diphenylated ketones. The yield was usually higher when the acidity of the medium was increased, which indicated the intermediate formation of the respective doubly-charged superelectrophile.[11,12] However, geminal double phenylation was only achieved when the electron deficiency of the starting material was high enough to react with benzene, which is most likely deactivated.

With only four π-electrons in total, diprotonated 2,3-butanedione is a small and outstanding candidate to study the conflicting effects of steric repulsion by the methyl groups and π-donation by the hydroxy groups, as it is one of the simplest possible vicinal carbon-centered superelectrophiles. Therefore, we investigated the conditions to generate and stabilize this compound. The results are reported herein.

Results and Discussion

Syntheses and Properties

Monoprotonated 2,3-butanedione $[C_2(O)(OH)Me_2]^+$ was isolated as the $[AsF_6]^-$ and $[SbF_6]^-$ salts by applying the superacidic systems HF/AsF_5 and HF/SbF_5 with one equivalent of the respective Lewis acid in anhydrous hydrogen fluoride (aHF) at −50 °C. The general equation is given below (Equation 1).

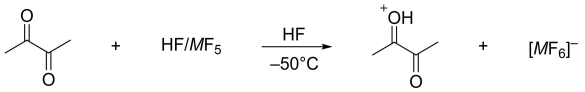

(1)

M = As, Sb

The isolation of the diprotonated species with a twofold amount of the mentioned Lewis acids did not succeed in aHF solution. When 2,3-butanedione is dissolved in aHF with two equivalents of SbF_5 at −70 °C, a variety of side products is detected. The ^{19}F NMR spectrum (Figure S3, Supporting Information) shows a quartet at −83.8 ppm, indicating the addition of fluorine to at least one of the central carbon atoms, despite the presence of excess Lewis acid. Another side product found in the same sample is $[H_3CCO]^+$, as evidenced in the Raman

[a] A. Virmani, C. Jessen, Prof. Dr. A. J. Kornath
Department Chemie
Ludwig-Maximilians-Universität München
Butenandtstraße 5–13 (D)
D-81377 München
E-mail: andreas.kornath@cup.uni-muenchen.de

Supporting information for this article is available on the WWW under https://doi.org/10.1002/chem.202400354

© 2024 The Authors. Chemistry - A European Journal published by Wiley-VCH GmbH. This is an open access article under the terms of the Creative Commons Attribution License, which permits use, distribution and reproduction in any medium, provided the original work is properly cited.

© 2024 The Authors. Chemistry - A European Journal published by Wiley-VCH GmbH

(Figure S1) and the ^{13}C NMR spectrum at −70 °C (Figure S4). The shifts occur at 146.9 ppm and 6.0 ppm as well as a Raman frequency at 2308 cm^{-1}.[13–15] When the solution is warmed up to room temperature, a singlet occurs at 182.0 ppm in the ^{13}C NMR spectrum (Figure S5) and is assigned to carbon monoxide,[16,17] indicating an HF-induced disproportionation of 2,3-butanedione.

In the course of our studies, we tried the diprotonation of 2,3-butanedione using the superacidic system HF/AsF_5 in aHF, but no quantitative diprotonation was observed. Instead, a ketal-like condensation product of the formula $[C_8H_{13}F_2O_3][AsF_6]$ crystallized from aHF within ten minutes at −45 °C. An attempted explanation, visualized in Scheme 1, is the AsF_5-induced addition of hydrogen fluoride to protonated 2,3-butanedione, increasing the nucleophilicity of the hydroxy group and allowing it to quickly react with another cation. The adduct formed then reacts further in a similar fashion. In the end, H_3O^+ is eliminated while formally adding another fluoride ion. The product was analyzed via single-crystal X-ray diffraction and is characterized in the Supporting Information.

To generate $[C_2(OH)_2Me_2]^{2+}$, 2,3-butanedione was dissolved with two equivalents of both HF and SbF_5 in SO_2 at −55 °C. The reaction is given in Equation 2. Employing SO_2 instead of aHF as a solvent turned out necessary to prevent the superelectrophile from reacting further. By changing the solvent, the protonating species is not H_2F^+ anymore, as it is in HF/SbF_5. The acidity of a superacidic system is limited to the acidity of the protonated solvent, which is in this case SO_2H^+. It was found that the removal of the solvent after mixing equimolar amounts of HF and SbF_5 in SO_2 is crucial to prevent the precipitation of $[FSO_2H][Sb_xF_{5x+1}]$ ($x = 1, 2$),[18] which drastically reduces the acidity of the system. For more details, see the Supporting Information.

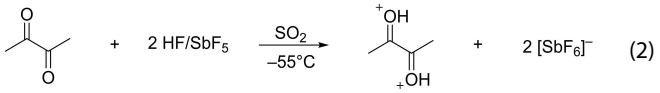

(2)

Raman Spectroscopy

Low-temperature Raman spectra of $[C_2(OH)_2Me_2][SbF_6]_2 \cdot 2\ SO_2$ and $[C_2(O)(OH)Me_2][AsF_6]$ are displayed in Figure 1. Selected

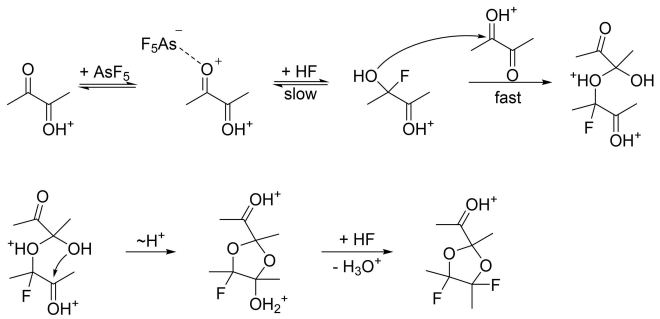

Scheme 1. Proposed mechanism of the formation of the ketal-like product from 2,3-butanedione with a twofold amount of AsF_5 in aHF.

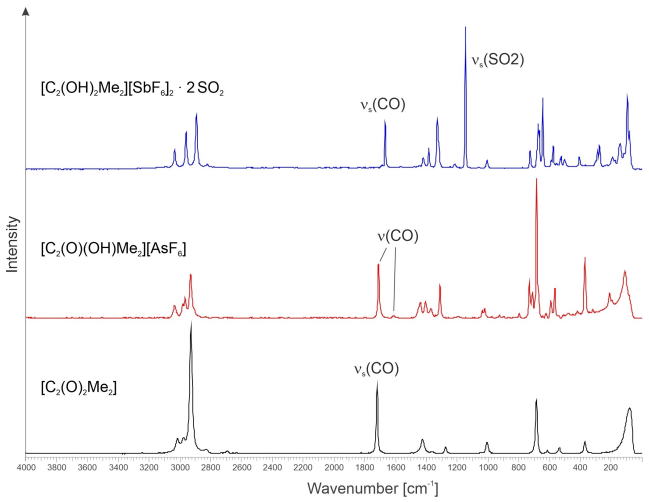

Figure 1. Stacked Raman spectra of 2,3-butanedione (bottom, black), $[C_2(O)(OH)Me_2][AsF_6]$ (middle, red), and $[C_2(OH)_2Me_2][SbF_6]_2 \cdot 2\ SO_2$ (top, blue).

experimental and quantum-chemically calculated frequencies (B3LYP/aug-cc-pVTZ) of the dication are listed in Table 1. For a full assignment, see Table S3 in the Supporting Information. The cation $[C_2(O)(OH)Me_2]^+$ exhibits C_s symmetry and has 21 A′ and 12 A″ fundamental vibrations according to quantum-chemical calculations, and is discussed in the Supporting Information.

The quantum-chemical optimization of the naked dication $[C_2(OH)_2Me_2]^{2+}$ reveals C_2 symmetry with a tilt of 37.48° around the central C–C bond. In the X-ray structure analysis discussed later, a planar C_{2h} geometry is observed. Another structure optimization including four HF molecules added to the dication to simulate donor-acceptor interactions revealed C_{2h} symmetry (see Theoretical Study below). Subsequently, the frequency analysis was performed. For C_{2h}, 36 fundamental vibrations ($\Gamma_{vib} = 12\ A_g + 7\ A_u + 6\ B_g + 11\ B_u$) of the dication are expected, of which all vibrations of the races A_g and B_g are Raman active, but IR inactive due to the rule of mutual exclusion.[19]

Compared to the starting material,[20,21] the symmetric CO stretching vibration is red-shifted from 1719 cm^{-1} to 1667 cm^{-1} as a result of the protonation, caused by the significant importance of the hydroxycarbenium resonance structure.[10,22] Furthermore, the stretching vibration of the central CC bond is red-shifted from 1288 cm^{-1} to 1216 cm^{-1}. On the other hand,

Table 1. Selected experimental and calculated vibrational frequencies of $[C_2(OH)_2Me_2]^{2+}$.

$[C_2(OH)_2Me_2][SbF_6]_2$ exp. Ra[b]	$[C_2(OH)_2Me_2]^{2+} \cdot 4$ HF calc.[a] (IR/Ra)	Assignment	
1667 (31)	1682 (0/19)	A_g	ν_s(CO)
1216 (2)	1232 (0/4)	A_g	ν(CC)
726 (12)	718 (0/10)	A_g	ν_s((H$_3$C)C)

[a] Calculated at the B3LYP/aug-cc-pVTZ level of theory. [b] Experimental Raman intensities are scaled to the most intensive line to be 100. [c] Abbreviations: ν = stretch, s = symmetric.

© 2024 The Authors. Chemistry - A European Journal published by Wiley-VCH GmbH

15213765, 0 Downloaded from https://chemistry-europe.onlinelibrary.wiley.com/doi/10.1002/chem.202400354, Wiley Online Library on [03/06/2024]. See the Terms and Conditions (https://onlinelibrary.wiley.com/terms-and-conditions) on Wiley Online Library for rules of use; OA articles are governed by the applicable Creative Commons License

$\nu_s((H_3C)C)$ occurs at 726 cm^{-1} and thus is blue-shifted with respect to the parent compound 2,3-butanedione (693 cm^{-1}).

For the anion $[SbF_6]^-$, more frequencies than expected are detected (Table S3). This results from a distorted O_h symmetry, as confirmed by the crystal structure analysis. The most intensive line at 1146 cm^{-1} is attributed to $\nu(SO_2)$ of SO_2 which co-crystallized in the solid state.[23]

Crystal Structure of $[C_2(OH)_2Me_2][SbF_6]_2 \cdot 2\ SO_2$

Single crystals of $[C_2(OH)_2Me_2][SbF_6]_2 \cdot 2\ SO_2$ were obtained by recrystallizing the colorless substance from a mixture of equal amounts of SO_2 and SO_2ClF at −70 °C. $[C_2(OH)_2Me_2][SbF_6]_2 \cdot 2\ SO_2$ crystallizes in the monoclinic space group $P2_1/c$ with four formula units per unit cell. The cation with short contacts is displayed in Figure 2, Table 2 contains selected structural details. The formula unit is given in Figure S1, and X-ray data and parameters are shown in Table S2 (see Supporting Information).

The C1–C2 bond with a distance of 1.443(4) Å shortens significantly compared to the starting material (1.476(6) Å).[24] The shortening of the C1–C2 bond of this dication is more pronounced than in other protonated ketones,[10,22] and even more comparable with fluorine-substituted carbenium ions.[25] Comparing the C1–C1*i* bond of $[C_2(OH)_2Me_2]^{2+}$ (1.549(4) Å) with that in parent 2,3-butanedione (1.540(6) Å),[24] surprisingly no significant difference can be noted. The distances are comparable to other non-conjugated $C(sp^2)$–$C(sp^2)$ bonds like oxalic acid and oxamide.[26,27] The C1–O1 distance extends from 1.209(6) Å[24] to 1.250(4) Å as a result of charge delocalization and is shorter than other protonated ketones.[22]

Regarding the bond angles of the cation, several significant changes relative to 2,3-butanedione are observed. The C2–C1–O1 angle widens slightly from 124.5(3)° to 126.9(2)° as a direct result of the protonation, enhancing the repulsion between oxygen and the methyl group.[24] Consequently, the angle O1–C1–C1*i* is decreased from 118.8(2)° to 111.7(2)°, whereas the C2–C1–C1*i* angle expands from 116.7(2)° to 121.3(2)°. These angles amount to approximately 360°, underlining the sp^2 hybridization of the central carbon atoms. The dihedral angles of 2.1(4)° and −2.1(4)° are close to a planar C_{2h} structure of the carboxo skeleton.

In the crystal packing, the $[C_2(OH)_2Me_2]^{2+}$ cation is surrounded by four anions, two of which form strong hydrogen bonds O1···F3 and O1*i*···F3*i* (Figure 2) with a distance of 2.476(3) Å. The other two anions are connected directly to the central carbon atoms, amounting to four C···F contacts in total. These interactions span a rhomboid with intermolecular distances of 2.520(3) Å (C1···F2*ii* and C1*i*···F2*iii*) and 2.625(4) Å (C1*i*···F2*ii* and C1···F2*iii*), which are approximately 21 % and 17 % less than the sum of the van-der-Waals radii (3.17 Å), respectively.[28]

The Sb–F bonds of the anion with distances between 1.857(3) Å and 1.928(2) Å are in good agreement with previously observed values.[29–32] The Sb1–F2 and Sb1–F3 bonds, which are involved in donor-acceptor interactions, are significantly longer than the other Sb–F bonds, resulting in a distortion of the ideal O_h symmetry. Co-crystallized SO_2 displays S–O bond lengths (both 1.425(3) Å) which are comparable to previously reported distances in literature.[33]

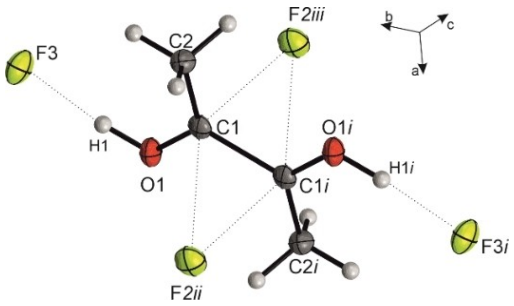

Figure 2. The dication of $[C_2(OH)_2Me_2][SbF_6]_2 \cdot 2\ SO_2$ with its short interionic contacts, which are visualized as dashed lines (50 % probability displacement ellipsoids). Symmetry operations: *i* = −*x*, −*y*, −*z*; *ii* = −*x*, 0.5 + *y*, 1.5−*z*; *iii* = *x*, 1.5−*y*, −0.5 + *z*.

Table 2. Selected bond distances, intermolecular interactions [Å], bond angles, and dihedral angles [°] of $[C_2(OH)_2Me_2][SbF_6]_2 \cdot 2\ SO_2$. Symmetry operations: *i* = −*x*, 2−*y*, 1−*z*; *ii* = −*x*, 0.5 + *y*, 1.5−*z*; *iii* = *x*, 1.5−*y*, −0.5 + *z*.

Bond lengths [Å]		Intermolecular interactions D(–H)···A [Å]	
C1–C1*i*	1.549(4)	C1···F2*ii*	2.520(3)
C1–C2	1.443(4)	C1···F2*iii*	2.625(4)
C1–O1	1.250(4)	O1(–H1)···F3	2.476(3)
Bond angles [deg]		**Dihedral angles [deg]**	
C2–C1–C1*i*	121.3(2)	O1–C1–C1*i*–O1*i*	−180.0(3)
C2–C1–O1	126.9(3)	C2–C1–C1*i*–C2*i*	180.0(3)
O1–C1–C1*i*	111.7(2)	C2–C1–C1*i*–O1*i*	−2.1(4)
		O1–C1–C1*i*–C2*i*	2.1(4)

Theoretical Study

Structure optimizations and vibrational frequencies were calculated by applying the DFT method B3LYP and the basis sets aug-cc-pVTZ and aug-cc-pVQZ, respectively. As mentioned earlier, the quantum-chemically calculated gas-phase structure of the naked dication $[C_2(OH)_2Me_2]^{2+}$ (B3LYP/aug-cc-pVQZ) has C_2 symmetry following from a tilt of 37.48° around the central C–C bond. However, as shown by the Raman spectroscopic and X-ray structure analyses, the cation exhibits C_{2h} symmetry. To evaluate the difference between these conformers, we first calculated the rotational scan around the central C–C bond of the naked cation on the B3LYP/aug-cc-pVTZ level of theory. The structure was optimized after every rotation of 1°, starting from a dihedral angle (C1–C2–C3–O2 and O1–C2–C3–C4, respectively) of 0°. The energy scan is displayed in Figure S15. The lowest energies were calculated for a dihedral angle of 36° and −36° (C_2 symmetry). After a rotation of 180°, the dication has C_s symmetry (syn position of the OH groups), representing the energy maximum with an energy difference of + 12.17 $kJ \cdot mol^{-1}$

© 2024 The Authors. Chemistry - A European Journal published by Wiley-VCH GmbH

15213765, 0 Downloaded from https://chemistry-europe.onlinelibrary.wiley.com/doi/10.1002/chem.202400354, Wiley Online Library on [03/06/2024]. See the Terms and Conditions (https://onlinelibrary.wiley.com/terms-and-conditions) on Wiley Online Library for rules of use; OA articles are governed by the applicable Creative Commons License

compared to the C_2 symmetric structure. The experimentally observed C_{2h} structure is represented at a local maximum at 0° with a small energy difference of $+0.79\ kJ \cdot mol^{-1}$.

The question arises as to why in the solid-state C_{2h} symmetry is formed, whereas the calculated optimization of the bare cation has a torsion angle of 37.48°. Either the cation is constrained into the C_{2h} symmetry by the crystal packing or intermolecular interactions have a stabilizing effect on the planar structure. Hence, for a more representative investigation, four HF molecules were added to the gas-phase structure of the dication to simulate donor-acceptor interactions, similar to the insights from the X-ray structure analysis. The complex was optimized at the B3LYP/aug-cc-pVTZ level of theory, revealing C_{2h} symmetry. This indicates a higher electronic occupancy of the p(π) orbitals of the central carbon atoms than without intermolecular contacts. To evaluate the individual interactions separately, we additionally calculated the optimized gas-phase structures of the cation with the two differently bonded HF molecules, hydrogen bridges and C···F interactions. The calculated structures are displayed in Figure 3.

The optimization of $[C_2(OH)_2Me_2]^{2+}$ with two hydrogen-bonded HF molecules exhibits dihedral angles of 35.60°. Hydrogen bridges were expected to reduce the oxonium character of the protonated keto groups, facilitating π-donation of the hydroxy groups. Yet, in our case, it only makes a difference of less than 2°. The optimization of the dication with two perpendicular HF molecules however exhibits a C1–C2–C3–O2 angle of 0.08° and an O1–C2–C3–C4 angle of −0.04°, thus very close to a planar structure. In conclusion, the energy gain by the electron donation into the central CC(π) bond solely by the C···F interactions is high enough to defy the sterical strain of the substituents.

To quantify this effect, we performed Natural Bond Orbital (NBO) calculations of the optimized structure of $[C_2(OH)_2Me_2]^{2+}$ with two perpendicular HF molecules at the MP2/aug-cc-pVTZ level of theory. The LUMO is represented by the two anti-bonding π*(C–O) orbitals and the bonding π(C–C) orbital, respectively (Figure 4). The occupation of both these orbitals (π*(C2–O1) and π*(C3–O2)) is 0.121 electrons.

The second-order perturbation theory analysis shows intra-molecular donor-acceptor interactions into the π*(C–O) orbitals that are identified as π-donation and σ-conjugation (Table 3 and Table S13). Interestingly, we find additional intermolecular interactions of the π(C–C) orbital with one lone pair of each of the coordinating fluorine atoms, displayed in Figure 4. For the F1 atom, stabilization energies of 16.7 (π*(C2–O1)) and 17.2 $kJ \cdot mol^{-1}$ (π*(C3–O2)) are calculated. For F2, the energies amount to 17.2 (π*(C2–O1)) and 16.7 $kJ \cdot mol^{-1}$ (π*(C3–O2)). The energy of this donor-acceptor interaction into the CC(π) bond sums up to 67.8 $kJ \cdot mol^{-1}$. It is thus nearly twice as big as the contribution of π-donation (36.8 $kJ \cdot mol^{-1}$), which was identified as the main source of stabilizing energy in previous theoretical investigations of the geometry of small carbon-centered superelectrophiles.[7]

To fathom the extreme electrophilicity of the dication, Molecular Electrostatic Potentials (MEP) are calculated at the MP2/aug-cc-pVTZ level of theory for the naked diprotonated species $[C_2(OH)_2Me_2]^{2+}$, constrained into a planar C_{2h} structure, and for the starting material for comparison. The MEPs are illustrated in Figure 5.

As 2,3-butanedione is already an electrophile, the highest positive electrostatic potential is located on the central C–C bond, while the methyl groups have a slightly less positive potential. The π-hole in the middle of the C–C bond has a calculated positive electrostatic potential of 108.4 $kJ \cdot mol^{-1}$. After diprotonation, the highest electrostatic potential is completely focused on the central carbon atoms, where it is

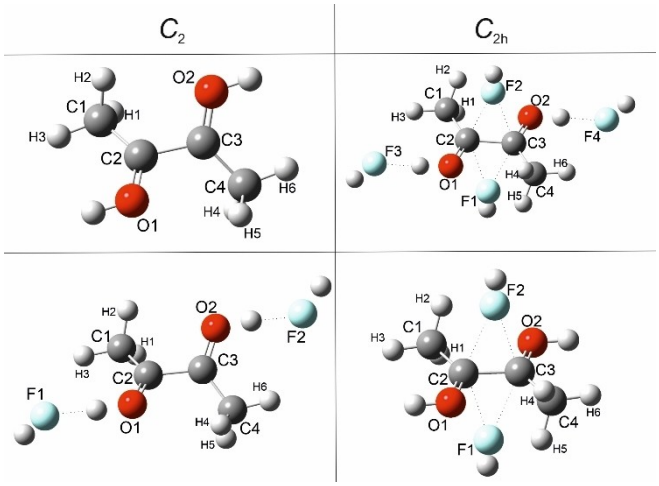

Figure 3. Optimized gas-phase structures of $[C_2(OH)_2Me_2]^{2+} \cdot n$ HF ($n = 0, 2, 4$). The left column shows calculated optimizations that reveal C_2 symmetry, and C_{2h} on the right. Calculated on the B3LYP/aug-cc-pVTZ level of theory.

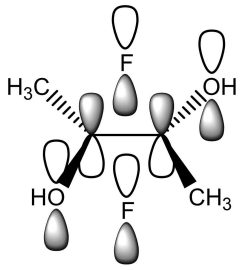

Figure 4. Intermolecular donor-acceptor interactions of two perpendicular HF molecules into the π(C–C) orbital. Hydrogen atoms of the HF ligands are omitted for clarity.

Table 3. Selected energies of donor-acceptor interactions from the second-order perturbation theory analysis of $[C_2(OH)_2Me_2]^{2+} \cdot 2$ HF. Calculated at the MP2/aug-cc-pVTZ level of theory.

Donor NBO	Acceptor NBO	Stabilizing energy [$kJ \cdot mol^{-1}$]	Assignment
π(C2–O1)	π*(C3–O2)	18.4	π-donation
π(C3–O2)	π*(C2–O1)	18.4	π-donation
n(F1)	π*(C2–O1)	16.7	Donor-acceptor interaction
n(F1)	π*(C3–O2)	17.2	Donor-acceptor interaction
n(F2)	π*(C2–O1)	17.2	Donor-acceptor interaction
n(F2)	π*(C3–O2)	16.7	Donor-acceptor interaction

© 2024 The Authors. Chemistry - A European Journal published by Wiley-VCH GmbH

15213765, 0 Downloaded from https://chemistry-europe.onlinelibrary.wiley.com/doi/10.1002/chem.202400354, Wiley Online Library on [03/06/2024]. See the Terms and Conditions (https://onlinelibrary.wiley.com/terms-and-conditions) on Wiley Online Library for rules of use; OA articles are governed by the applicable Creative Commons License

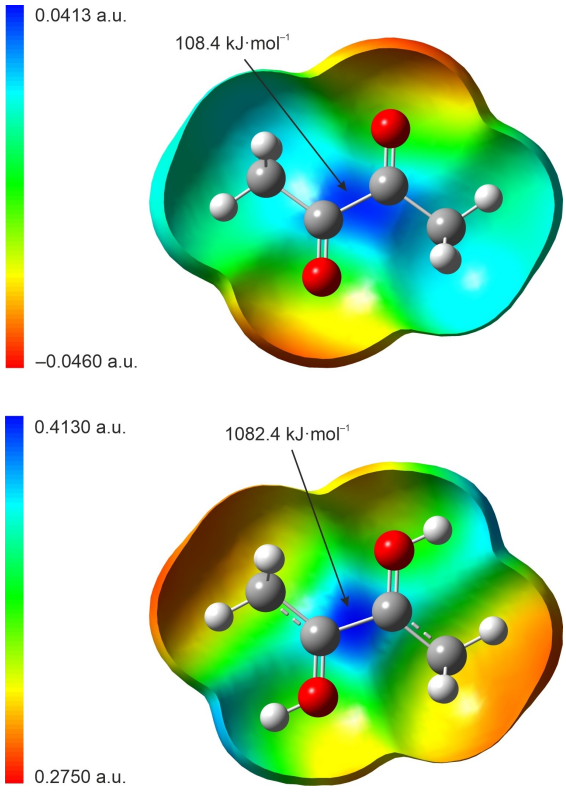

Figure 5. Molecular 0.0004 bohr^{-3} 3D isosurfaces with mapped electrostatic potential as a color scale from −0.0460 a.u. (red) to 0.0413 a.u. (blue) for 2,3-butanedione (top) and from 0.2750 a.u. (red) to 0.4130 a.u. (blue) for the diprotonated species (bottom).

even higher than at the protons added to the system. This π-hole directly above the C–C bond has an electrostatic potential of 1082.4 kJ·mol^{-1}. As shown in the X-ray structure analysis, the C–C bond of $[C_2(OH)_2Me_2]^{2+}$ remains unchanged compared to the starting material, despite an approximately tenfold increase in the π-hole. Considering this, the intermolecular C···F interactions seem to play a crucial role in the stabilization of the superelectrophile.

Conclusions

The synthesis of the simple superelectrophile $[C_2(OH)_2Me_2]^{2+}$ in condensed phase by diprotonation of 2,3-butanedione is presented. The compound undergoes side reactions in anhydrous hydrogen fluoride and thus cannot be stabilized in convenient superacids, the usage of SO_2 as a solvent turned out crucial. The isolated product is analyzed by Raman spectroscopy and single-crystal X-ray diffraction. The central C–C bond length of the superelectrophile cannot be distinguished from the starting material and is stabilized by intermolecular C···F interactions. MEP calculations quantify the extreme electrophilicity, and NBO analyses show that this hyperconjugation found in the solid state has a significant influence on the geometry of the dication, which is to the best of our knowledge the smallest vicinal, carbon-centered superelectrophile analyzed to date in the solid state.

Experimental Section

Caution! Avoid contact with any of these materials. Hydrogen fluoride will be formed by the hydrolysis of these compounds. HF burns the skin and causes irreparable damage. Safety precautions should be taken when using and handling these materials.

Apparatus and materials. All reactions were carried out at standard Schlenk conditions by using FEP/PFA reactors closed with a stainless-steel valve and a stainless-steel vacuum line. All vessels have been dried with fluorine prior to use. Raman spectroscopic analyses were rendered at −196 °C with a Bruker MultiRAM FT-Raman spectrometer with an Nd:YAG laser excitation up to 1000 mW (λ = 1064 nm) in a usable range between 50 cm^{-1} and 4000 cm^{-1}. Single-crystal X-ray structure investigations were carried out with an Oxford Xcalibur3 diffractometer equipped with a Spellman generator (50 kV, 40 mA) and a KappaCCD detector. The measurements were performed with Mo-K_α radiation (λ = 0.71073 Å). For data collection, the software CrysAlis CCD,[34] for data reduction the software CrysAlis RED[35] was used. The solution and refinement were performed with the programs SHELXT[36] and SHELXL-97[37] implemented in the WinGX software package[38] and checked with the software PLATON.[39] The absorption correction was achieved with the SCALE3 ABSPACK multi-scan method.[40] Quantum-chemical calculations were performed with the Gaussian 09[41] and the Gaussian 16[42] program package. Calculations were carried out employing the B3LYP functional and the basis sets aug-cc-pVTZ and aug-cc-pVQZ. NBO calculations were performed on the MP2/aug-cc-pVTZ level of theory. For visualization of the structures and vibrational modes, the program GaussView 6.0[43] was employed. NMR spectra were recorded either on a Jeol ECX400 NMR or a Bruker AV400 NMR instrument. The spectrometers were externally referenced to $CFCl_3$ for ^{19}F and to tetramethylsilane for ^{1}H and ^{13}C NMR spectra. The spectra were recorded inside 4 mm FEP NMR tube inliners. Acetone-*d6* was employed for external shimming when aHF was used as a solvent for the respective compounds. 2,3-Butanedione (Aldrich) was used as purchased, antimony pentafluoride (VWR) was distilled three times prior to use. Arsenic pentafluoride was synthesized from the elements and purified by fractionated distillation.

Deposition Numbers 2123235 (for $[C_2(OH)_2Me_2][SbF_6]\cdot 2\ SO_2$) and 2123236 (for $[C_8H_{13}F_2O_3][AsF_6]$) contain the supplementary crystallographic data for this paper. These data are provided free of charge by the joint Cambridge Crystallographic Data Centre and Fachinformationszentrum Karlsruhe Access Structures service.

Acknowledgements

Financial support of this work by the Ludwig-Maximilian University Munich (LMU), the Deutsche Forschungsgemeinschaft (DFG), and F-Select GmbH is gratefully acknowledged. Open Access funding enabled and organized by Projekt DEAL.

Conflict of Interests

The authors declare no conflict of interest.

© 2024 The Authors. Chemistry - A European Journal published by Wiley-VCH GmbH

15213765, 0 Downloaded from https://chemistry-europe.onlinelibrary.wiley.com/doi/10.1002/chem.202400354, Wiley Online Library on [03/06/2024]. See the Terms and Conditions (https://onlinelibrary.wiley.com/terms-and-conditions) on Wiley Online Library for rules of use; OA articles are governed by the applicable Creative Commons License

Data Availability Statement

The data that support the findings of this study are available in the supplementary material of this article.

Keywords: donor-acceptor interactions · quantum chemical calculations · superacidic systems · superelectrophile · X-ray diffraction

[1] T. Ohwada, K. Shudo, *J. Am. Chem. Soc.* **1989**, *111*, 34.
[2] D. A. Klumpp, *Chem. Eur. J.* **2008**, *14*, 2004.
[3] G. Frenking, W. Koch, H. Schwarz, *J. Comput. Chem.* **1986**, *7*, 406.
[4] K. Lammertsma, M. Barzaghi, G. A. Olah, J. A. Pople, A. J. Kos, P. v. R. Schleyer, *J. Am. Chem. Soc.* **1983**, *105*, 5252.
[5] R. H. Nobes, M. W. Wong, L. Radom, *Chem. Phys. Lett.* **1987**, *136*, 299.
[6] G. Hossein Shafiee, *OJPC* **2012**, *02*, 176.
[7] G. Frenking, *J. Am. Chem. Soc.* **1991**, *113*, 2476.
[8] G. A. Olah, *Superelectrophiles and their chemistry*, Wiley-Interscience, Hoboken, N.J, **2008**.
[9] G. K. S. Prakash, T. N. Rawdah, G. A. Olah, *Angew. Chem. Int. Ed. Engl.* **1983**, *22*, 390.
[10] A. Virmani, M. Pfeiffer, C. Jessen, Y. Morgenstern, A. J. Kornath, *Z. Anorg. Allg. Chem.* **2022**, *14*, e202200005.
[11] T. Ohwada, T. Yamazaki, T. Suzuki, S. Saito, K. Shudo, *J. Am. Chem. Soc.* **1996**, *118*, 6220.
[12] T. Yamazaki, S. Saito, T. Ohwada, K. Shudo, *Tetrahedron Lett.* **1995**, *36*, 5749.
[13] G. A. Olah, A. M. White, *J. Am. Chem. Soc.* **1967**, *89*, 7072.
[14] G. A. Olah, A. M. White, *J. Am. Chem. Soc.* **1969**, *91*, 5801.
[15] P. N. Gates, D. Steele, *J. Mol. Struct.* **1968**, *1*, 349.
[16] J. B. Stothers, *Appl. Spectrosc.* **1972**, *26*, 1.
[17] J. Firl, W. Runge, *Angew. Chem. Int. Ed. Engl.* **1973**, *12*, 668.
[18] A. Kornath, R. Seelbinder, R. Minkwitz, *Angew. Chem. Int. Ed.* **2005**, *44*, 973.
[19] P. F. Bernath, *Spectra of Atoms and Molecules*, Oxford University Press, Oxford, **2016**.
[20] J. R. Durig, S. E. Hannum, S. C. Brown, *J. Phys. Chem.* **1971**, *75*, 1946.
[21] A. Gómez-Zavaglia, R. Fausto, *J. Mol. Struct.* **2003**, *661–662*, 195.
[22] D. Stuart, S. D. Wetmore, M. Gerken, *Angew. Chem. Int. Ed.* **2017**, *56*, 16380.
[23] A. Anderson, R. Savoie, *Can. J. Chem.* **1965**, *43*, 2271.
[24] K. Eriks, T. D. Hayden, S. H. Yang, I. Y. Chan, *J. Am. Chem. Soc.* **1983**, *105*, 3940.
[25] K. O. Christe, X. Zhang, R. Bau, J. Hegge, G. A. Olah, G. K. S. Prakash, J. A. Sheehy, *J. Am. Chem. Soc.* **2000**, *122*, 481.
[26] J. L. Derissen, P. H. Smith, *Acta Crystallogr., Sect. B: Struct. Sci.* **1974**, *30*, 2240.
[27] G. de With, S. Harkema, *Acta Crystallogr., Sect. B: Struct. Sci.* **1977**, *33*, 2367.
[28] A. Bondi, *J. Phys. Chem.* **1964**, *68*, 441.
[29] R. Minkwitz, A. Kornath, R. Krause, H. Preut, *Z. Anorg. Allg. Chem.* **1994**, *620*, 632.
[30] R. Minkwitz, C. Hirsch, *Z. Anorg. Allg. Chem.* **1999**, *625*, 1674.
[31] R. Minkwitz, S. Schneider, *Angew. Chem. Int. Ed.* **1999**, *38*, 210.
[32] M. Schickinger, T. Saal, F. Zischka, J. Axhausen, K. Stierstorfer, Y. Morgenstern, A. J. Kornath, *ChemistrySelect* **2018**, *3*, 12396.
[33] S. Grabowsky, P. Luger, J. Buschmann, T. Schneider, T. Schirmeister, A. N. Sobolev, D. Jayatilaka, *Angew. Chem. Int. Ed.* **2012**, *51*, 6776.
[34] CrysAlisCCD, *Version 1.171.35.11 (release 16–05-2011 CrysAlis 171.NET)*, Oxford Diffraction Ltd, UK, **2011**.
[35] CrysAlisRED, *Version 1.171.35.11 (release 16–05-2011 CrysAlis 171.NET)*, Oxford Diffraction Ltd, UK, **2011**.
[36] G. M. Sheldrick, *Acta Crystallogr., Sect. A: Found. Adv.* **2015**, *71*, 3.
[37] G. M. Sheldrick, *SHELXL-97, Program for Crystal Structure Solution*, University of Göttingen, Germany, **1997**.
[38] L. J. Farrugia, *J. Appl. Crystallogr.* **1999**, *32*, 837.
[39] A. L. Spek, *PLATON, A Multipurpose Crystallographic Tool*, Utrecht University, Utrecht, Netherlands, **1999**.
[40] *SCALE3 ABSPACK, An Oxford Diffraction Program*, Oxford Diffraction Ltd, UK, **2005**.
[41] M. J. Frisch, G. W. Trucks, H. B. Schlegel, G. E. Scuseria, M. A. Robb, J. R. Cheeseman, G. Scalmani, V. Barone, B. Mennucci, G. A. Petersson, H. Nakatsuji, M. Caricato, X. Li, H. P. Hratchian, A. F. Izmaylov, J. Bloino, G. Zheng, J. L. Sonnenberg, M. Hada, M. Ehara, K. Toyota, R. Fukuda, J. Hasegawa, M. Ishida, T. Nakajima, Y. Honda, O. Kitao, H. Nakai, T. Vreven, J. A. Montgomery, J. E. Peralta, F. Ogliaro, M. Bearpark, J. J. Heyd, E. Brothers, K. N. Kudin, V. N. Staroverov, R. Kobayashi, J. Normand, K. Raghavachari, A. Rendell, J. C. Burant, S. S. Iyengar, J. Tomasi, M. Cossi, N. Rega, J. M. Millam, M. Klene, J. E. Knox, J. B. Cross, V. Bakken, C. Adamo, J. Jaramillo, R. Gomperts, R. E. Stratmann, O. Yazyev, A. J. Austin, R. Cammi, C. Pomelli, J. W. Ochterski, R. L. Martin, K. Morokuma, V. G. Zakrzewski, G. A. Voth, P. Salvador, J. J. Dannenberg, S. Dapprich, A. D. Daniels, O. Farkas, J. B. Foresman, J. V. Ortiz, J. Cioslowski, D. J. Fox, *Gaussian09, Revision A.02*, Gaussian, Inc., Wallingford CT, **2009**.
[42] M. J. Frisch, G. W. Trucks, H. B. Schlegel, G. E. Scuseria, M. A. Robb, J. R. Cheeseman, G. Scalmani, V. Barone, G. A. Petersson, H. Nakatsuji et al., *Gaussian 16 Rev. C.01*, Wallingford, CT, **2016**.
[43] Roy Dennington, Todd A. Keith, John M. Millam, *GaussView 6*, Semichem Inc., Shawnee Mission KS, **2019**.

Manuscript received: January 27, 2024
Accepted manuscript online: February 19, 2024
Version of record online: ■■, ■■

© 2024 The Authors. Chemistry - A European Journal published by Wiley-VCH GmbH

15213765, 0, Downloaded from https://chemistry-europe.onlinelibrary.wiley.com/doi/10.1002/chem.202400354, Wiley Online Library on [03/06/2024]. See the Terms and Conditions (https://onlinelibrary.wiley.com/terms-and-conditions) on Wiley Online Library for rules of use; OA articles are governed by the applicable Creative Commons License

RESEARCH ARTICLE

The synthesis of the small superelectrophile $[C_2(OH)_2Me_2]^{2+}$ turned out to be a challenging task since stabilizing it in convenient superacids was not possible. Quantum chemical calculations predict a reduced C_2 symmetry, yet experimental data confirms C_{2h} symmetry in the solid state. The origin of this finding is fathomed based on X-ray structure analysis together with quantum chemical calculations.

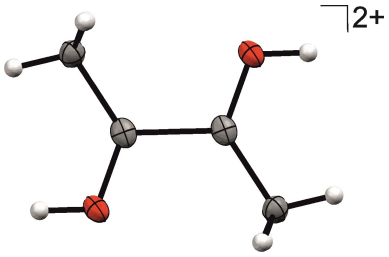

*A. Virmani, C. Jessen, Prof. Dr. A. J. Kornath**

15213765, 0, Downloaded from https://chemistry-europe.onlinelibrary.wiley.com/doi/10.1002/chem.202400354, Wiley Online Library on [03/06/2024]. See the Terms and Conditions (https://onlinelibrary.wiley.com/terms-and-conditions) on Wiley Online Library for rules of use; OA articles are governed by the applicable Creative Commons License